

Lensing of Gravitational Waves as a Novel Probe of Graviton Mass

Adrian Ka-Wai Chung*

*Theoretical Particle Physics and Cosmology Group, Department of Physics,
King's College London, University of London, Strand, London, WC2R 2LS, U.K.*

Tjonnie G.F. Li†

*Department of Physics, The Chinese University of Hong Kong, Shatin, N.T., Hong Kong
Institute for Theoretical Physics, KU Leuven, Celestijnenlaan 200D, B-3001 Leuven, Belgium and
Department of Electrical Engineering (ESAT), KU Leuven,
Kasteelpark Arenberg 10, B-3001 Leuven, Belgium*

The diffraction patterns of lensed gravitational waves encode information about their propagation speeds. If gravitons have mass, the dispersion relation and speed of gravitational waves will be affected in a frequency-dependent manner, which would leave potentially detectable traces in the diffraction pattern if the waves are lensed. In this paper, we study how the alternative dispersion relation induced by massive gravitons affects gravitational waves lensed by point-mass lenses, such as intermediate-mass black holes. By detecting a single lensed gravitational-wave signal, we can measure the graviton mass with an accuracy better than the combined measurement across $\mathcal{O}(10^2)$ unlensed signals. Our method can be generalised to other lens types, gravitational-wave sources, and detector networks, opening up new ways to measure the graviton mass through gravitational-wave detection.

I. INTRODUCTION

When gravitational waves propagate near a massive compact object, the propagation direction will be changed due to the gravity of the compact object [23, 28, 48, 54–56]. This phenomenon is known as lensing. The lensed waves interfere amongst themselves to form new wave patterns. The lensing pattern depends on the nature of the lens, lensing geometry, and interference between different (possible) rays. Lensing is a crucial astrophysical probe. For example, lensing of gravitational waves might provide us with the information of the existence of intermediate-mass black holes (of mass $\sim 10^2 M_\odot - 10^3 M_\odot$) [38], cosmological expansion [27, 33] and testing general relativity [26, 30, 45, 46]. Since the direct detection of gravitational waves, searches for lensed gravitational waves has been popular [22, 32, 44]. Nonetheless, no conclusive evidence of lensed gravitational-wave signals has been found as of the time of writing.

Another popular aspect of studies is the dispersion relation of gravitational waves [4–16, 18, 21]. According to general relativity, gravitational waves are local Lorentz invariant, obeying the dispersion relation of $\omega = ck$, where ω is the angular frequency, c is the speed of light, and k is the wavenumber. This dispersion relation implies that gravitons are massless. If the gravitons have mass, gravitational waves obey an alternative dispersion relation, leading to different propagation speeds for various frequencies. As gravitational waves propagate, dephasing will be developed across different frequencies.

By (not) detecting the dephasing, we can constrain the graviton mass. As of the time of writing, no evidence of significant Lorentz violation has been found using this method [8, 9, 12, 15]. Alternatively, the near-field behaviour of black holes has also been suggested as a probe of the graviton mass [25].

The graviton mass might also be encoded in lensed gravitational waves. The dispersion relation of gravitational waves due to the massive graviton will change the time delay of waves of different frequencies in different directions, leading to additional features of the resultant lensing pattern. These additional features open up a whole new possibility of measuring the graviton mass by detecting lensed gravitational waves. Moreover, the amplification of gravitational-wave signal by lensing may help to improve the measurement accuracy of the graviton mass. Measuring the graviton mass by lensing also makes relevant tests more complete because lensing involves the strength of gravity intermediate between the near and far-field. In this paper, we propose a novel method to measure graviton mass by detecting lensed gravitational waves.

Throughout the paper, m_g is in unit of $c = \hbar = 1$ (so $h = 2\pi$), while the mass of compact objects (such as black hole and lens) are in unit of $c = G = 1$.

II. LENSING PATTERN OF GRAVITATIONAL WAVES WITH DISPERSION

A. Assumptions and approximations

This work makes a few assumptions.

1. Following [34, 37, 42], we ignore the screening of gravity due to the mass of graviton [51]. This assumption implies that we will ignore the effects on

* ka-wai.chung@ligo.org

† tgfli@cuhk.edu.hk

the dynamics of binary black hole mergers due to the graviton mass. In the context of lensing, this assumption implies that at a sufficiently far distance r , the Newtonian gravitational potential due to a black hole (point-mass lens) of mass M is given by $\frac{M}{r}$.

2. We focus only on the effects on GW lensing due to the graviton mass. Other consequences of lensing, such as modification on polarization [35] and phase shift [40, 41], will be omitted. These are acceptable approximations because including these effects will include more contrasting features to graviton-mass measurement. In this work, we focus on improvements on the constraint or measurement accuracy of the graviton mass by considering the combined effects of lensing and dephasing induced by the graviton mass.

B. Method

If gravitons have mass, phenomenologically, the dispersion relation of gravitational waves will be altered to [42],

$$\omega^2 = k^2 + m_g^2, \quad (1)$$

where m_g is the mass of graviton¹. If $m_g \ll k$, the propagation speed of dispersive gravitational waves that obey this dispersion relation can be approximated by the following equation,

$$v_g(f) \approx 1 - \frac{1}{8\pi^2} \frac{m_g^2}{f^2}. \quad (2)$$

When propagating in a flat space-time, the dispersive gravitational waves obeying Eq. (1) will acquire a dephasing due to the difference in propagation speeds among different frequencies [42],

$$\Psi_{\text{disp}}(f; m_g) = -\frac{\pi D_0}{\lambda_g^2} \frac{1}{(1+z)f}, \quad (3)$$

where $\lambda_g = 1/m_g$ is Compton's wavelength of the graviton, D_0 is the propagation distance from the source to the detector and z is the redshift of the source binary. Thus, in the frequency domain, the waveform of unlensed dispersive gravitational waves is

$$\tilde{h}_{\text{disp}}(f) = \tilde{h}(f)e^{i\Psi_{\text{disp}}(f)}, \quad (4)$$

where $\tilde{h}(f)$ is the original (unlensed) GR waveform (see, e.g., [3, 24, 49], for GR waveform approximants).

When encountering a massive compact object, such as an intermediate-mass black hole, gravitational waves will be lensed. The lensing effect is characterized by the amplification function (or transmission factor) [29, 53], F , which is the ratio of lensed-wave amplitude to unlensed-wave amplitude,

$$\tilde{h}_L(f) = F(f)\tilde{h}(f), \quad (5)$$

where $\tilde{h}_L(f)$ is the lensed waveform and $\tilde{h}(f)$ is the unlensed waveform. Given a lensing geometry, $F(f)$ can be computed by [47, 54, 56]

$$F(f; \vec{\theta}_s) = \frac{D_L D_S}{D_{LS}} \xi_0^2 \frac{(1+z_L)}{i} \frac{f}{v_g} \times \int d^2\vec{\theta}_L \exp \left[2\pi i f t_d(\vec{\theta}_L, \vec{\theta}_s) \right], \quad (6)$$

where v_g is GW propagation speed, D_L, D_S and D_{LS} are respectively the lens-to-observer distance, the source-to-observer distance and the source-to-lens distance, z_L is the redshift of lens, $\vec{\theta}_s$ is the displacement from optical axis to the source on source plane, $\vec{\theta}_L$ is the displacement from optical axis to lens on lens plane, t_d is the time delay between the lensed ray and unlensed ray,

$$t_d(\vec{\theta}, \vec{\theta}_s) = \frac{(1+z_L)}{v_g} \left[\frac{D_L D_S}{2D_{LS}} |\vec{\theta}_s - \vec{\theta}|^2 - \psi(\vec{\theta}_s) \right], \quad (7)$$

where $\psi(\vec{\theta}_s)$ is the lensing potential. Overall t_d also depends on $v_g, \vec{\theta}_s$ and lens $\vec{\theta}_L$ and ξ_0 is a length scale.

We note that the amplification function Eq. (6) depends on $\frac{f}{v_g}$ as a whole. Thus, the amplification function of GWs of the massive graviton is just that of GWs without dispersion with the following replacement,

$$f \rightarrow \beta(f)f, \quad (8)$$

where

$$\beta(f) = \frac{c}{v_g(f)} \approx 1 + \frac{1}{2} \frac{m_g^2}{f^2}. \quad (9)$$

As a proof-of-principle demonstration, in this work we focus on the case of a point mass lens, such as a black hole. For a point-mass lens, the amplification function can be analytically evaluated as [54, 56]

$$F(f; M_{\text{len}}, y, m_g) = \exp \left(\frac{\pi}{4} w \beta \right) \left(\frac{w}{2} \beta \right)^{i\frac{w}{2}\beta} \Gamma \left(1 - i\frac{w}{2}\beta \right) {}_1F_1 \left(i\frac{w}{2}\beta, 1; i\frac{w}{2}\beta y^2 \right), \quad (10)$$

where M_{len} is the redshifted mass of the lens and y is the impact parameter of lensing, Γ is the (complex) Gamma function, ${}_1F_1$ is confluent hypergeometric function, $w = 8\pi M_{\text{len}} f$ is the dimensionless frequency. The resulting

¹ Alternatively, this equation can be interpreted as a definition of the massive graviton which leads to the dispersion of gravitational perturbations. In this work, we refer "the mass of graviton" to m_g defined by Eq. (1)

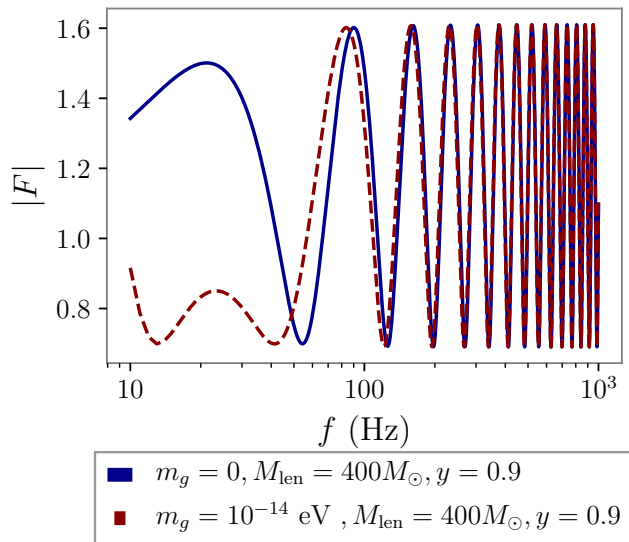


FIG. 1. The lensing amplification function due to an intermediate mass black hole of redshifted mass $M_{\text{lens}} = 400 M_{\odot}$ at $y = 0.9$ corresponding to $m_g = 0$ (solid blue line) and $m_g = 10^{-14} \text{eV}$ (dashed red line).

lensed waveform of gravitational waves corresponding to the massive gravitons can be written as

$$\tilde{h}_L(f; m_g) = F(f; M_{\text{lens}}, y, m_g) \tilde{h}(f) e^{i\Psi_{\text{disp}}(f)}. \quad (11)$$

Note that, according to Eq. (2), gravitational waves of different frequencies are different. The only constant achromatic speed is the speed of light. Therefore, the effects described by Eq. (11) is not degenerate with a constant change of propagation speed of gravitational waves. Thus, the effects of the massive gravitons can be distinguished upon gravitational-wave detection.

Fig. 1 plots $F(f)$ corresponding to the lensing by an intermediate mass black hole of redshifted lens mass $M_{\text{lens}} = 400 M_{\odot}$ and $y = 0.9$ for $m_g = 0$ and $m_g = 10^{-14} \text{eV}$ as a function of f . The modifications to the lensing pattern due to the dispersion relation Eq. (1) are most manifest in the low-frequency regime ($f \leq 100 \text{Hz}$), corresponding to the energy scale of $hf \sim m_g c^2$. As the frequency of gravitational waves increases, the changes to the amplification function due to the alternative dispersion become increasingly less manifest because the ultra-relativistic limit $E \approx p$ has been attained.

III. PARAMETER ESTIMATION

A. Bayesian Inference

Eq. (10) suggests that, upon detecting a GW signal lensed by a point-mass lens, we can measure (or constrain) m_g along with other lensing parameters and the

parameters describing the source binary. We denote parameters describing the source binary by $\vec{\theta}_{\text{BBH}}$ and parameters describing the lens by $\vec{\theta}_{\text{lens}} = (M_{\text{lens}}, y)$. By Bayes' theorem, the posterior of m_g , $\vec{\theta}_{\text{lens}}$ and $\vec{\theta}_{\text{BBH}}$ is given,

$$p(\vec{\theta}_{\text{BBH}}, \vec{\theta}_{\text{lens}}, m_g | \tilde{d}, H, I) \propto p_{\text{BBH}}(\vec{\theta}_{\text{BBH}} | H, I) p_{\text{lens}}(\vec{\theta}_{\text{lens}} | H, I) p_m(m_g | H, I) \times p(\tilde{d} | \vec{\theta}_{\text{BBH}}, \vec{\theta}_{\text{lens}}, m_g, H, I), \quad (12)$$

where $p_{\text{BBH}}(\vec{\theta}_{\text{BBH}} | H, I)$, $p_{\text{lens}}(\vec{\theta}_{\text{lens}} | H, I)$ and $p_m(m_g | H, I)$ are respectively the prior of $\vec{\theta}_{\text{BBH}}$, $\vec{\theta}_{\text{lens}}$ and m_g . Since $\vec{\theta}_{\text{BBH}}$, $\vec{\theta}_{\text{lens}}$ and m_g should be independent, we have assumed that their priors are factorized. $p(\tilde{d} | \vec{\theta}_{\text{BBH}}, \vec{\theta}_{\text{lens}}, m_g, H, I)$ is the likelihood that a binary black hole of $\vec{\theta}_{\text{BBH}}$ and lens of $\vec{\theta}_{\text{lens}}$ will generate detected strain data \tilde{d} ,

$$p(\tilde{d} | m_g, \vec{\theta}_{\text{lens}}, \vec{\theta}_{\text{BBH}}, \vec{\theta}, H, I) \propto \exp \left(-2 \sum_{D=H,L,V} \int_0^{+\infty} df \frac{|\tilde{h}_D(m_g, \vec{\theta}_{\text{lens}}, \vec{\theta}_{\text{BBH}}) - \tilde{d}_D|^2}{S_D(f)} \right), \quad (13)$$

where $\tilde{h}_D(m_g, \vec{\theta}_{\text{lens}}, \vec{\theta}_{\text{BBH}})$ is the frequency-domain response corresponding to detector D by the waveform Eq. (11) and $S_D(f)$ the one-sided power-spectral density of a given detector D (H, L, V for Hanford, Livingston and Virgo, respectively).

Following [38], we place a uniform prior for M_{lens} . For y , we place a prior which is uniform for $y^2 \in [0, 1]$ instead of y . For m_g , we place a prior which is uniform for $\log_{10} m_g \in [-26, -20]$, which covers the magnitude of the most updated constraints on m_g [21] by gravitational waves and small enough values for us to explore constraints tighter than the known constraints. Although for this range of m_g the modification to the lensed gravitational waveform by m_g is dominated by the dephasing $\Psi_{\text{disp}}(f; m_g)$, it is still interesting for us to investigate how the amplification of a signal by lensing can help measure or constrain m_g . At last, the marginalized posterior of m_g can be obtained by marginalizing Eq. (12) over $\vec{\theta}_{\text{BBH}}$ and $\vec{\theta}_{\text{lens}}$,

$$p(m_g | \tilde{d}, H, I) = \int d\vec{\theta}_{\text{BBH}} \int d\vec{\theta}_{\text{lens}} p(\vec{\theta}_{\text{BBH}}, \vec{\theta}_{\text{lens}}, m_g | \tilde{d}, H, I). \quad (14)$$

To gauge possible improvements of the measurement accuracy of m_g by a lensed signal over unlensed signal(s), we will compare the posterior of m_g due to the simulated lensed signal with its unlensed counterpart (henceforth labelled as “unlensed signal”). However, lensing-rate calculations suggest that the Advanced LIGO and Virgo detectors will detect a lensed signal per ~ 600 unlensed signals [36]. Thus, a more fair comparison will be with the posterior of m_g combined across ~ 600 unlensed signals.

However, in practice, the combined measurement accuracy of m_g will be dominated by the signal with the best measurement accuracy. For an unlensed signal, there are two factors significantly affecting the measurement (or constraint) accuracy of m_g . One is the signal-to-noise ratio (SNR). The other is the propagation distance (see Eq. (3)). Thus, we first simulated a population of ~ 600 binary black-hole mergers according to [20], each of which has an SNR of ≥ 10 , approximately the minimum SNR for an event to be detectable by the Advanced LIGO and Virgo detectors [19, 21, 43]. Then, we look for the source with the furthest distance whose SNR is still larger than 30 to estimate the optimal measurement accuracy. We represent the measurement of m_g combined across these 600 simulated signals by the posterior of m_g of this signal (henceforth labelled as “population signal”).

B. Mock signals of $m_g = 0$

We first apply our analysis to mock signals of $m_g = 0$. We prepare unlensed signals in the frequency domain by the IMRPhenoPv2 template [3, 49], a phenomenological waveform template calibrated against numerical-relativity simulations, using the LALSimulation library [39]. The simulated unlensed signals contain the inspiral, merger and ringdown phase. Expressly, for both the lensed and unlensed signal (but not the population signal), we assume a source binary black hole whose parameters are close to that of GW150914, the first detected gravitational-wave event [6]. The originally unlensed signal corresponds to an SNR of 46, and the SNR of the population signal corresponds to 30.

We then map the unlensed signal into the lensed signal by multiplying the frequency-domain waveform by the amplification function Eq. (6). For the lensed signal, we assume that the signal is lensed by an intermediate-mass black hole of reshifted mass $400M_\odot$ and lensing parameter $y = 0.9$. This mass of lens is chosen because intermediate-mass black holes of similar masses are hoped to be discovered by gravitational-wave lensing [38]. This value of y is chosen because it is more likely to have a larger y (see the prior of y). After being lensed, the SNR of the signal is boosted to 57. The prepared signals are injected into simulated Gaussian noise assuming the design sensitivity of the Advanced LIGO and Virgo detectors [1, 2]. When inferring the lensed signal, we use the waveform model of Eq. (11) with the dephasing due to massive graviton included. For the unlensed signal, we infer with the waveform model with $F(f; m_g)$ in Eq. (11) set to be 1 for all frequency and M_{lens} and y are removed from inference. The diagonal Fig. 2 shows the posterior of redshifted lens mass M_{lens} , y and $\log m_g$ and the off-diagonal plots show the two-dimensional posterior distributions amongst the variables. The green vertical lines mark the injected values. The red vertical line marks the 3σ interval of the marginalized posterior of $\log_{10} m_g$ from $m_g = 10^{-26}\text{eV}$. From Fig. 2, we find that the posterior

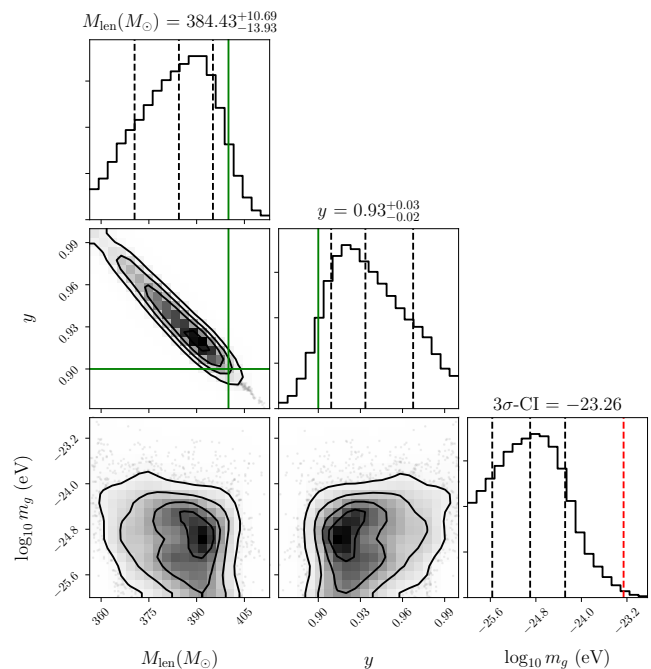


FIG. 2. The corner plot shows the marginalized posterior of the redshifted lens mass M_{lens} , y and $\log m_g$ and their correlations, although we also infer the parameters of the source binary together as free parameters. The posteriors are estimated from a mock lensed signal due to a source binary black hole of $68M_\odot$ at a luminosity distance of 400 Mpc lensed by a black hole of $400M_\odot$ at $y = 0.9$. The green lines denote the injected values for M_{lens} and y . The red line on the marginalized posterior of $\log_{10} m_g$ denotes the 3σ confidence interval (90-CI) from the lower limit of the prior of $\log_{10} m_g$. We conclude that we can constraint the graviton mass while accurately measuring the lensing-related parameters.

of $\log_{10} m_g$ has no support for $\log_{10} m_g > -23.2$ because our measurement of gravitational waves rules out the possibility of an excessive large m_g . From the posterior of M_{lens} and y , we conclude that we can accurately estimate the lensing-related parameters while testing the graviton mass with lensing. Moreover, judging from Fig. 2 there are no strong correlations between the lensing-related parameters and m_g .

To study the changes in measurement accuracy due to lensing, we overlay the posterior of $\log_{10} m_g$ of the lensed signal (solid blue line) and its unlensed counterpart (dashed red line) in Fig. 3. The 3σ interval of the unlensed signal (dashed vertical line) is -22.9 , corresponding to $m_g \sim 1.3 \times 10^{-23}\text{eV}$. Similarly, the 3σ interval of the “population” signal is $\log_{10} m_g \sim -22.9$ ². The 3σ CI of the lensed signal is -23.3 , corresponding to $m_g \sim 5 \times 10^{-24}\text{eV}$, about half of the constraints by unlensed signals. Our results suggest that a single lensed

² We notice that the marginalized posterior of $\log_{10} m_g$ of the population signal is slightly bipolar. This is because the log likeli-

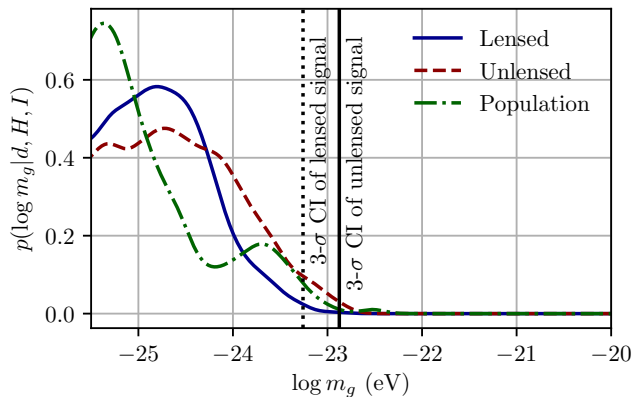


FIG. 3. The marginalized posterior of m_g in solid blue line is obtained from a lensed signal due to a GW150914-like binary lensed by a black hole of $M_{\text{len}} \approx 400M_{\odot}$ at $y = 0.9$. To gauge the improvement of the constraint, we compare the result of a lensed signal with its unlensed counterpart (dashed red line). Moreover, lensing rate calculations suggest that the Advanced LIGO and Virgo may detect a lensed signal per ~ 600 unlensed signals. For a fair comparison, we also compare the lensed result with the best constraint likely to be obtained from 600 simulated unlensed signals (dotted green line, dubbed “population” signal). The solid vertical line denotes the 3σ confidence interval (CI) of the posterior of $\log m_g$ of the unlensed signal ($\sim -22.9 \Rightarrow m_g \sim 10^{-23}$ eV) and the dashed vertical line denotes the 3σ -CI of the lensed signal ($\sim -23.3 \Rightarrow m_g \sim 5 \times 10^{-24}$ eV). The constraint due to the lensed signal is more stringent than that by the unlensed signal and the population signal.

signal can lead to a constraint on m_g tighter than that combined across $\mathcal{O}(10^2)$ unlensed signal.

C. Mock signals of $m_g \sim 3 \times 10^{-23}$ eV

We also perform our test on lensed and unlensed mock signals of $m_g \sim 3 \times 10^{-23}$ eV, approximately the constraints on m_g by various astrophysical observations [16, 19, 21]. The source binary black holes, lensing geometry and simulations of mock signals are the same as described in Section III B.

hood (Eq. (13)) contains a term proportional to

$$\langle \tilde{h}_0 | \tilde{h} \rangle = \frac{4}{T} \sum_{D,i} \frac{|\tilde{h}_0(f_i)|^2}{S_D(f_i)} \cos\left(\frac{\pi D_0}{\lambda_g^2(1+z)f_i}\right), \quad (15)$$

where T is the signal duration, \tilde{h}_0 is the injected waveform of $m_g = 0$ and $\tilde{h} = \tilde{h}_0 \exp(i\Psi_{\text{disp}}(f; m_g))$ is the waveform model with m_g as a parameter. As m_g increases, the argument inside the cosine function monotonically increases, but $\langle \tilde{h}_0 | \tilde{h} \rangle$ is not monotonically decreasing because of the oscillatory properties of the cosine term. For a longer propagation distance D_0 , the oscillatory properties will be more manifest because the argument changes more sensitively with m_g .

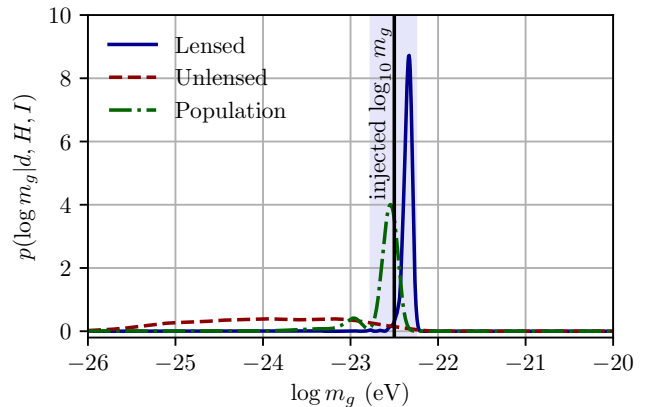


FIG. 4. The marginalized posterior of m_g of lensed (solid blue), unlensed signals (dashed red) and the population signal (dashed-dotted red). For all signals, we assume $m_g = 10^{-22.5}$ eV $\sim 3 \times 10^{-23}$ eV. We assume a GW150914-like source binary black hole generates the lensed and unlensed signal. The “population” signal is generated according to the description in Fig. 3 and the main text. The lens is the same of that considered in Fig. 3 and Section III B. The solid vertical line marks the injected $\log_{10} m_g$. The shaded region denotes the 3σ confidence interval of the posterior obtained from the lensed signal.

Fig. 4 shows the posterior of $\log_{10} m_g$ obtained from the simulated lensed and unlensed signals. The posterior of $\log m_g$ of the unlensed signal (dashed red line) is much broader than that of the lensed signal (solid blue line). Although the posterior of the unlensed signal is consistent with the injected m_g , from which we cannot confidently draw any conclusive evidence of the existence of massive graviton. The population signal (in dashed-dotted green line) gives a posterior which peaks at the injected $\log_{10} m_g$ with larger support. The lensed signal gives a posterior of m_g , which peaks more sharply at a value close to the injected m_g . From the posteriors, we read (within 3σ interval) $\log_{10} m_g = -22.3_{-0.432}^{+0.112}$ from the lensed signal, $\log_{10} m_g = -23.9_{-2.01}^{+1.64}$ from the original unlensed signal and $\log_{10} m_g = -22.7_{-3.30}^{+0.356}$ from the “population” signal. The width of the posterior of the lensed signal is approximately smaller than a tenth of that of the unlensed counterpart and one-third of that of the population signal, which suggests that a single lensed signal can lead to measurement of the graviton mass more accurate than the combined measurement across $\mathcal{O}(10^2)$ unlensed signals. Our results demonstrate the novel ability of lensed gravitational-wave signals to significantly improve the graviton mass’s measurement accuracy.

IV. CONCLUDING REMARKS

This paper studies the lensing pattern by a point-mass lens of gravitational waves with an isotropic dispersion

relation due to massive gravitons. We find that a massive graviton changes the lensing pattern of gravitational waves, especially for gravitational waves of wavelength comparable with Compton's wavelength of the considered graviton mass. Most importantly, we demonstrate that by detecting a lensed gravitational-wave signal, we can measure the graviton mass with an accuracy better than the combined measurement across $\mathcal{O}(10^2)$ unlensed signals. We expect that our analysis can be applied to real detection when the Advanced LIGO and Virgo detect a lensed signal in the future.

Other than the improvement of measurement accuracy of the graviton mass, our method enjoys several advantages. Firstly, compared to other proposed methods of testing the speed of GWs by observing lensing [26, 30], our approach requires no observation of the electromagnetic counterpart(s) of a given event. Therefore, our method is more stand-alone and is easier to be performed. Secondly, our method is independent of the nature of the source binaries. Although in this paper, we focused on gravitational waves generated by binary black holes, our method can be straightforwardly applied to other types of coalescence, such as binary neutron star coalescence [50]. Binary neutron-star coalescence has been detected at a relatively close luminosity distance ($\sim 50\text{Mpc}$) [12, 17], which may limit its ability to constrain graviton mass via measuring propagation dephasing (c.f. Eq. (3)). However, if gravitational waves generated by binary neutron star are lensed, these gravitational-wave events constraints can be significantly improved. This flexibility greatly extends the scope of graviton-mass measurement. Lastly, our method makes the test of graviton mass more complete. While the far-field propagation of gravitational waves [37, 42] and near-field behaviour of black holes [25] have been proposed to constrain the mass of graviton, our test bridges the intermediate region between these two tests. Along with other tests of general relativity via observing the lensing of gravitational waves (such as [31]), our test demonstrates the strong potential to understand the nature of space-time via observing lensing.

In this work, we ignore the effects of (i) the change of polarization of gravitational waves due to lensing [35], (ii) the change of the behaviour of the source compact binary due to massive graviton, as is the case in [8, 15], and (iii) the change of the gravitational field around the lens by

the graviton mass. Also, our study focusing on the case of point mass lens. These ignored effects and the lensing of dispersive gravitational wave of other lens types remain fully explored. If we include these effects in our measurement, the accuracy can be further enhanced. Other than these effects, we plan to study the lensing of dispersive gravitational waves by lenses with structures, such as singular isothermal sphere (SIS), because their lensing pattern might vary more sensitively to the graviton mass, thereby further improving the measurement accuracy. We would also like to investigate the performance of our test for the detection by proposed space-based detectors, such as the Laser Interferometer Space Antenna (LISA) [52], which are capable of exquisite phase measurement and much better constraints. Therefore, in the future, we can measure the graviton mass with unparalleled accuracy by observing lensed gravitational-wave signals.

ACKNOWLEDGEMENT

The authors are indebted to valuable discussion among the lensing working group of LIGO. AKWC would like to acknowledge Patrick C.K. Cheong, Srashti Goyal and Shasvath Kapadia for stimulating discussions, Jose Maria Ezquiaga Bravo, Mark H.Y. Cheung, Otto A. Hannuksela, Alvin K.Y. Li and Ignacio Magana for their comments on the manuscript and relevant presentations and Robin S.H. Yuen for his advice about computer programming. AKWC was supported by the Hong Kong Scholarship for Excellence Scheme (HKSES). This work is partially supported by [Grand Number]. This manuscript carries a report number of KCL-PH-TH 2021/41 and LIGO Document number of P2100192-v2.

This research has made use of data, software and/or web tools obtained from the Gravitational Wave Open Science Center (<https://www.gw-openscience.org>), a service of LIGO Laboratory, the LIGO Scientific Collaboration and the Virgo Collaboration. LIGO is funded by the U.S. National Science Foundation. Virgo is funded by the French Centre National de Recherche Scientifique (CNRS), the Italian Istituto Nazionale della Fisica Nucleare (INFN) and the Dutch Nikhef, with contributions by Polish and Hungarian institutes.

[1] <https://dcc.ligo.org/LIGO-P1200087-v42/public>.

[2] <https://dcc.ligo.org/LIGO-T2000012/public>.

[3] P. Ajith, M. Hannam, S. Husa, Y. Chen, B. Brügmann, N. Dorband, D. Müller, F. Ohme, D. Pollney, C. Reisswig, L. Santamaría, and J. Seiler. Inspiral-merger-ringdown waveforms for black-hole binaries with non-precessing spins. *Phys. Rev. Lett.*, 106:241101, Jun 2011.

[4] B. P. Abbott *et al.*. Binary black hole mergers in the first advanced ligo observing run. *Phys. Rev. X*, 6:041015, Oct

2016.

[5] B. P. Abbott *et al.*. Gw151226: Observation of gravitational waves from a 22-solar-mass binary black hole coalescence. *Phys. Rev. Lett.*, 116:241103, Jun 2016.

[6] B. P. Abbott *et al.*. Observation of gravitational waves from a binary black hole merger. *Phys. Rev. Lett.*, 116:061102, Feb 2016.

[7] B. P. Abbott *et al.*. Properties of the Binary Black Hole Merger GW150914. *prl*, 116(24):241102, June 2016.

- [8] B. P. Abbott *et al.*. Tests of general relativity with gw150914. *Phys. Rev. Lett.*, 116:221101, May 2016.
- [9] B. P. Abbott *et al.*. Gw170104: Observation of a 50-solar-mass binary black hole coalescence at redshift 0.2. *Phys. Rev. Lett.*, 118:221101, Jun 2017.
- [10] B. P. Abbott *et al.*. Gw170608: Observation of a 19 solar-mass binary black hole coalescence. *The Astrophysical Journal Letters*, 851(2):L35, 2017.
- [11] B. P. Abbott *et al.*. Gw170814: A three-detector observation of gravitational waves from a binary black hole coalescence. *Phys. Rev. Lett.*, 119:141101, Oct 2017.
- [12] B. P. Abbott *et al.*. Gw170817: Observation of gravitational waves from a binary neutron star inspiral. *Phys. Rev. Lett.*, 119:161101, Oct 2017.
- [13] B. P. Abbott *et al.*. Prospects for Observing and Localizing Gravitational-Wave Transients with Advanced LIGO, Advanced Virgo and KAGRA. *Living Rev. Rel.*, 21:3, 2018. [Living Rev. Rel.19,1(2016)].
- [14] B. P. Abbott *et al.*. Gwtc-1: A gravitational-wave transient catalog of compact binary mergers observed by ligo and virgo during the first and second observing runs. *Phys. Rev. X*, 9:031040, Sep 2019.
- [15] B. P. Abbott *et al.*. Tests of general relativity with the binary black hole signals from the ligo-virgo catalog gwtc-1. *Phys. Rev. D*, 100:104036, Nov 2019.
- [16] B. P. Abbott *et al.*. GW190412: Observation of a Binary-Black-Hole Coalescence with Asymmetric Masses. *arXiv e-prints*, page arXiv:2004.08342, April 2020.
- [17] B. P. Abbott *et al.*. GW190425: Observation of a Compact Binary Coalescence with Total Mass $\sim 3.4 M_{\odot}$. *apjl*, 892(1):L3, March 2020.
- [18] B. P. Abbott *et al.*. GW190814: Gravitational waves from the coalescence of a 23 solar mass black hole with a 2.6 solar mass compact object. *The Astrophysical Journal*, 896(2):L44, jun 2020.
- [19] B. P. Abbott *et al.*. GWTC-2: Compact Binary Coalescences Observed by LIGO and Virgo During the First Half of the Third Observing Run. *arXiv e-prints*, page arXiv:2010.14527, October 2020.
- [20] B. P. Abbott *et al.*. Population Properties of Compact Objects from the Second LIGO-Virgo Gravitational-Wave Transient Catalog. *arXiv e-prints*, page arXiv:2010.14533, October 2020.
- [21] B. P. Abbott *et al.*. Tests of General Relativity with Binary Black Holes from the second LIGO-Virgo Gravitational-Wave Transient Catalog. *arXiv e-prints*, page arXiv:2010.14529, October 2020.
- [22] B. P. Abbott *et al.*. Search for lensing signatures in the gravitational-wave observations from the first half of LIGO-Virgo's third observing run. *arXiv e-prints*, page arXiv:2105.06384, May 2021.
- [23] Haugan Mark P Bontz, Robert J. A diffraction limit on the gravitational lens effect. *Astrophysics and Space Science*, August 1981.
- [24] Alessandra Buonanno, Bala R. Iyer, Evan Ochsner, Yi Pan, and B. S. Sathyaprakash. Comparison of post-newtonian templates for compact binary inspiral signals in gravitational-wave detectors. *Phys. Rev. D*, 80:084043, Oct 2009.
- [25] Adrian Ka-Wai Chung and Tjonnie Guang Feng Li. Phenomenological inclusion of alternative dispersion relations to the teukolsky equation and its application to bounding the graviton mass with gravitational-wave measurements. *Phys. Rev. D*, 99:124023, Jun 2019.
- [26] T. E. Collett and D. Bacon. Testing the Speed of Gravitational Waves over Cosmological Distances with Strong Gravitational Lensing. *Physical Review Letters*, 118(9):091101, March 2017.
- [27] Paolo Cremonese, Jose María Ezquiaga, and Vincenzo Salzano. Breaking the mass-sheet degeneracy with gravitational wave interference in lensed events. *arXiv e-prints*, page arXiv:2104.07055, April 2021.
- [28] S. Deguchi and W. D. Watson. Diffraction in Gravitational Lensing for Compact Objects of Low Mass. *Astrophys. J.*, 307:30, August 1986.
- [29] P. Schneider J. Ehlers E.E. Falco. *Gravitational Lenses*. Springer-Verlag Berlin Heidelberg, 1992.
- [30] X.-L. Fan, K. Liao, M. Biesiada, A. Piórkowska-Kurpas, and Z.-H. Zhu. Speed of Gravitational Waves from Strongly Lensed Gravitational Waves and Electromagnetic Signals. *Physical Review Letters*, 118(9):091102, March 2017.
- [31] Srashti Goyal, K. Haris, Ajit Kumar Mehta, and Parameswaran Ajith. Testing the nature of gravitational-wave polarizations using strongly lensed signals. *arXiv e-prints*, page arXiv:2008.07060, August 2020.
- [32] O. A. Hannuksela, K. Haris, K. K. Y. Ng, S. Kumar, A. K. Mehta, D. Keitel, T. G. F. Li, and P. Ajith. Search for Gravitational Lensing Signatures in LIGO-Virgo Binary Black Hole Events. *apjl*, 874(1):L2, March 2019.
- [33] Otto A. Hannuksela, Thomas E. Collett, Mesut Çalıřkan, and Tjonnie G. F. Li. Localizing merging black holes with sub-arcsecond precision using gravitational-wave lensing. *mnras*, 498(3):3395–3402, August 2020.
- [34] D. Hansen, N. Yunes, and K. Yagi. Projected constraints on Lorentz-violating gravity with gravitational waves. *Phys. Rev. D*, 91(8):082003, April 2015.
- [35] Shaoqi Hou, Xi-Long Fan, and Zong-Hong Zhu. Gravitational lensing of gravitational waves: Rotation of polarization plane. *Phys. Rev. D*, 100:064028, Sep 2019.
- [36] Tjonnie G. F. Li Ken K. Y. Ng, Kaze W. K. Wong and Tom Broadhurst. Precise ligo lensing rate predictions for binary black holes. *Phys. Rev. D*, 2017.
- [37] D. Keppel and P. Ajith. Constraining the mass of the graviton using coalescing black-hole binaries. *Phys. Rev. D*, 82:122001, Dec 2010.
- [38] Kwun-Hang Lai, Otto A. Hannuksela, Antonio Herrera-Martín, Jose M. Diego, Tom Broadhurst, and Tjonnie G. F. Li. Discovering intermediate-mass black hole lenses through gravitational wave lensing. *Phys. Rev. D*, 98(8):083005, October 2018.
- [39] LIGO Scientific Collaboration. LIGO Algorithm Library - LALSuite. free software (GPL), 2018.
- [40] Jose María Ezquiaga, Daniel E. Holz, Wayne Hu, Macarena Lagos, and Robert M. Wald. Phase effects from strong gravitational lensing of gravitational waves. *arXiv e-prints*, page arXiv:2008.12814, August 2020.
- [41] Jose María Ezquiaga and Miguel Zumalacárregui. Gravitational wave lensing beyond general relativity: birefringence, echoes and shadows. *arXiv e-prints*, page arXiv:2009.12187, September 2020.
- [42] S. Mirshekari, N. Yunes, and C. M. Will. Constraining Lorentz-violating, modified dispersion relations with gravitational waves. *Phys. Rev. D*, 85(2):024041, January 2012.
- [43] C. J. Moore, R. H. Cole, and C. P. L. Berry. Gravitational-wave sensitivity curves. *Classical and Quantum Gravity*, 32:015014, Jan 2015.

- [44] Suvodip Mukherjee, Tom Broadhurst, Jose M. Diego, Joseph Silk, and George F. Smoot. Inferring the lensing rate of LIGO-Virgo sources from the stochastic gravitational wave background. *mnras*, 501(2):2451–2466, February 2021.
- [45] Suvodip Mukherjee, Benjamin D. Wandelt, and Joseph Silk. Multimessenger tests of gravity with weakly lensed gravitational waves. *Phys. Rev. D*, 101(10):103509, May 2020.
- [46] Suvodip Mukherjee, Benjamin D. Wandelt, and Joseph Silk. Probing the theory of gravity with gravitational lensing of gravitational waves and galaxy surveys. *mnras*, 494(2):1956–1970, May 2020.
- [47] Takahiro T. Nakamura and Shuji Deguchi. Wave optics in gravitational lensing. *Progress of Theoretical Physics Supplement*, 133:137–153, 1999.
- [48] Hans C. Ohanian. On the focusing of gravitational radiation. *International Journal of Theoretical Physics*, June 1974.
- [49] Yi Pan, Alessandra Buonanno, Andrea Taracchini, Lawrence E. Kidder, Abdul H. Mroué, Harald P. Pfeiffer, Mark A. Scheel, and Béla Szilágyi. Inspiral-merger-ringdown waveforms of spinning, precessing black-hole binaries in the effective-one-body formalism. *Phys. Rev. D*, 89:084006, Apr 2014.
- [50] Peter T. H. Pang, Otto A. Hannuksela, Tim Dietrich, Giulia Pagano, and Ian W. Harry. Lensed or not lensed: determining lensing magnifications for binary neutron star mergers from a single detection. *mnras*, 495(4):3740–3750, May 2020.
- [51] Scott Perkins and Nicolás Yunes. Probing screening and the graviton mass with gravitational waves. *Classical and Quantum Gravity*, 36(5):055013, March 2019.
- [52] Travis Robson, Neil J Cornish, and Chang Liug. The construction and use of lisa sensitivity curves. *Classical and Quantum Gravity*, 36(10):105011, 2019.
- [53] P. Schneider. *Introduction to Gravitational Lensing and Cosmology*, pages 1–89. Springer Berlin Heidelberg, Berlin, Heidelberg, 2006.
- [54] R. Takahashi. Arrival Time Differences between Gravitational Waves and Electromagnetic Signals due to Gravitational Lensing. *Astrophys. J.*, 835:103, January 2017.
- [55] Ryuichi Takahashi and Takashi Nakamura. Wave Effects in the Gravitational Lensing of Gravitational Waves from Chirping Binaries. *Astrophys. J.*, 595(2):1039–1051, October 2003.
- [56] Ryuichi Takahashi and Takashi Nakamura. Wave effects in the gravitational lensing of gravitational waves from chirping binaries. *The Astrophysical Journal*, 595(2):1039, 2003.